

STUDY OF THE PHENOMENON OF THE INTERACTION BETWEEN SESSILE DROPS DURING EVAPORATION

Dorra KHILIFI^{1,4}, Walid FOU DHIL^{1,3}, Kamel FAHEM¹, Souad HARMAND², Sadok BEN JABRALLAH^{1,3}*

^{*1} Laboratory of Energetics and Thermal and Mass Transfer (LETTM), Science Faculty of Tunis, University of Tunis El Manar, 1060 Tunis, Tunisia

² University Lille Nord de France, F-59000 Lille, UVHC, LAMIH, F-59313 Valenciennes, France

³ University of Carthage, Science Faculty of Bizerte, 7021 Bizerte, Tunisia

⁴ University of Tunis El Manar, Science Faculty of Tunis, 1060 Tunis, Tunisia

* Corresponding author; E-mail: khelifidorrafst@gmail.com

This research work represents an experimental study of the interaction between water drops deposited on a substrate at ambient temperature. To examine this phenomenon, the evaporation of a single drop deposited on a substrate was first investigated. Then, several drops were deposited alongside on the same substrate under the same conditions. The central drop dynamic behavior was also examined and compared with that of a single drop. This comparison shows the effect of the interaction between the neighboring drops, which delayed the evaporation of these drops and particularly the central droplet, on evaporation. In fact, three configurations were studied by changing the initial distance (d) between the drops ($d = 0.2$ mm, $d = 7$ mm and $d = 15$ mm). The obtained results reveal that the interaction phenomenon becomes less important by increasing the distance between the drops. This is important for optimizing many industrial applications, such as spray drying, fuel injection in combustion engines, and other applications.

Key words: Deposited Drop, Evaporation, relative humidity, liquid-gas interface and Interaction.

1. Introduction

Evaporation of a drop deposited on a substrate is considered as a complex phenomenon during which several processes, such as the Marangoni effect, mass and thermal transfers, interact. This phenomenon was widely dealt with in many research works because of its intensive application in various fields as spray drying, DNA mapping [1-2], Inkjet printing [3-4], combustion engineering [5-6-7], electronic cooling [8], cooling system [9], etc.

For instance, authors, in [10-11], studied the evaporation of a sessile drop. They proved that the substrate thermo-physical properties can significantly affect the evaporation rate.

Besides, Lopes et al. [10] examined the influence of the substrate thermal properties (glass and silicone) on the evaporation time of the water droplets. They showed that evaporation, in the case of silicon, is faster than that in the case of a glass substrate due to its high thermal conductivity.

Numerous studies were also carried out on the evaporation modes of a sessile drop [13-14-15]. They revealed the existence of three behavioral modes of the sessile drop evaporation. The first mode is characterized by the reduction of the contact angle and the anchoring of the contact line (constant contact line mode). However, the second mode is characterized by the decrease of the contact line and the stabilization of the contact angle (constant contact angle mode); whereas the third mode, called stick-slip mode [16], is characterized by

minimizing the angle contact and the contact line simultaneously. The last mode was observed during the evaporation of different liquids [17-18-19] especially with the presence of nano-particles [20-21].

Moreover, several works demonstrated that, at the liquid-gas interface, the surface tension varies as a function of temperature. This variation involves the Marangoni forces investigated by many authors.

Lu et al. [22] examined the Marangoni effect on temperature evolution versus time at the liquid-vapor interface and at the upper surface of the substrate.

Yan et al. [23] proved that the role of Marangoni is more evident for the large values of the initial contact angle.

Ouenzerfi et al. [24] presented an experimental study on the inversion of the Marangoni effect of a drop of binary mixture (97% water - 3% butanol) under a horizontal temperature gradient. They showed that a binary drop (97% water - 3% butanol) tends to move to warmer areas.

Pin et al. [25] used an acoustic method to track the alcohol concentration at the bottom of a droplet of binary solution during the evaporation process.

However, conducting a numerical simulation of droplet evaporation is not an easy task, mainly because of the coupling of heat and mass transfer processes with the evolution of the free surface. To avoid the tracing of the free interface, some previous numerical simulation studies[26-27] focused on the evaporation at certain contact angle and contact line (fixed droplet profile), while others simulated the droplet volume variation as a function of time by decoupling the interface evolution with an evaporation calculation[28-29-30-31].

In fact, the flow evaporated at the liquid-gas interface was the subject of several research works.

For example, Widjaja et al. [32] studied a profile of the flow evaporated at the liquid-gas interface, showing that the evaporation is more intense near the triple line.

Galvin et al. [33] demonstrated that the concentration of saturated vapor above the liquid-gas interface depends on the droplet curvature.

To our knowledge, the literature taking place have focused on understanding the transfer phenomena of evaporation of a drop but in practice, applications involving several drops on the same substrate. The interaction between the drop does not extrapolate the results of a drop. The study of the evaporation of a drop surrounded by several drops is needed to examine the effect of the interaction between them: this is the subject of this work. To show the effects of the presence of several drops, the work has a section dedicated to the evaporation of a drop and a second portion where the drop will be surrounded by six other neighboring drops.

2. Experimental process

The sapphire substrate was placed in a controlled room ($14 \times 12.4 \times 7.5 \text{ cm}^3$) with temperature $T_{\text{amb}} = 21^\circ \text{C}$ and humidity $H = 50 \%$ (Figure 1). The water drop having initial temperature $T_0 = 20^\circ \text{C}$ and $0.7 \mu\text{l}$ volume was deposited on the sapphire substrate using a programmable syringe (KdScientific legato 100), resulting in a deposit drop diameter of about 1.5 mm.

Obviously, there was no air movement inside the room whose upper part was equipped with an infrared transparent sapphire window to allow measuring the temperature at the drop surface using the infrared camera (FLIR X6580SC, 640×512 pixels, $15 \mu\text{m}$ detector pitch) . The room was also equipped with a hole for the syringe passage.

A Kruss-shape analyzer was employed to measure the drop contact angle, its volume, its diameter and its height during evaporation. A side view CCD camera (Allied Vision Technologies, 780×580 pixels) was utilized to record the process of the drop evaporation.

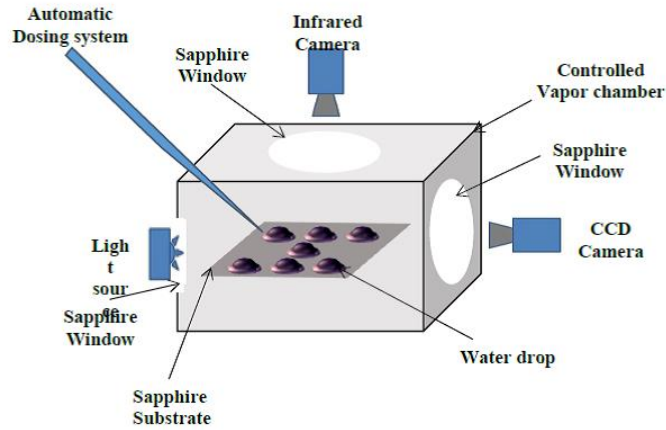


Fig.1. Schema of the experimental setup

3. Experimental results

3.1 Description of the evaporation of a single drop of water on a substrate

In this part, we will study the single drop sessile on a sapphire substrate.

Figure 2 and Figure 3 show respectively the variations of the volume, the contact angle and the drop diameter over time.

In fact, the drop volume decreased over time. The drop, evaporating on the sapphire, had a constant diameter for almost half of the drop life, while the contact angle minimized linearly over time. Two evaporation stages were observed (Stage 1): during this stage, the drop evaporated according to a constant contact line mode. After about 450 s, the diameter began to diminish linearly, while the contact angle remained constant for a period $\Delta t = 350$ s (Stage 2): the drop evaporated in a constant contact angle mode.

Stage (III): during this stage, the drop deposited on the substrate exhibited a different behavior in which the diameter and the contact angle were reduced simultaneously until the drop disappeared totally, which represents the stick slip mode.

Figure 4 demonstrates the evolution of the evaporated density over time. Indeed, the evaporated density attained its maximum value at $t = 0$ s because the concentration gradient ($c_{\text{sat}}, c_{\text{amb}}$) was important at $t = 0$ s. Obviously, at the beginning of evaporation, the air, in the drop immediate vicinity, became wetter and temperature decreased at the liquid-gas interface. This behavior was due to the effect of the interface cooling by evaporation which led to a considerable decline in the concentration gradient ($c_{\text{sat}}, c_{\text{amb}}$) and explained the decrease in the evaporated density over time.

The drop images taken at different times reveal of the drop evaporation (Fig.5). In this figure, we present the process of the water drop evaporation until its total disappearance. We notice, from the experiment, that the life of this water drop is was around 820 s.

At the beginning of evaporation, to become relatively constant, the liquid-gas interface temperature did not require long time. Then, it decreased relatively at the end of the evaporation due to the interface cooling by evaporation.

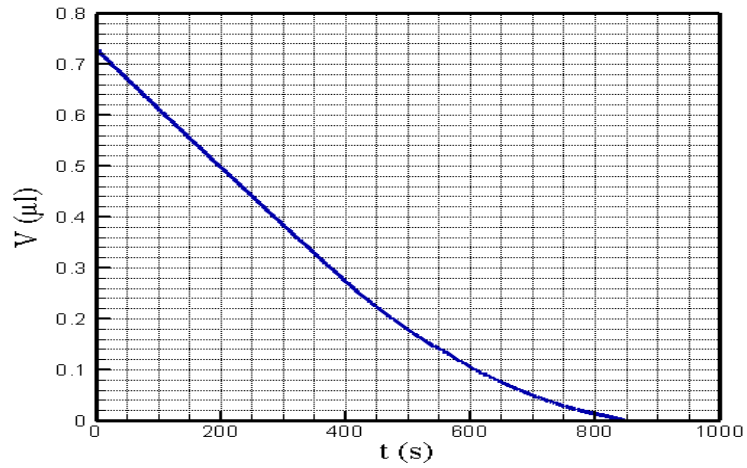


Fig.2. Variations in the volume of drop as function of time at: $T_{amb} = 21 \text{ }^\circ\text{C}$ and $H = 50 \%$

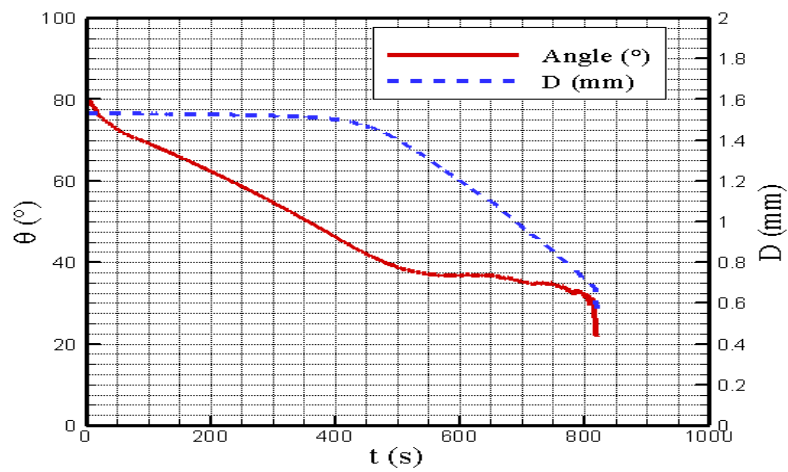


Fig.3 Variations in the contact angle and diameter of drop as function of time at: $T_{amb} = 21 \text{ }^\circ\text{C}$ and $H = 50 \%$

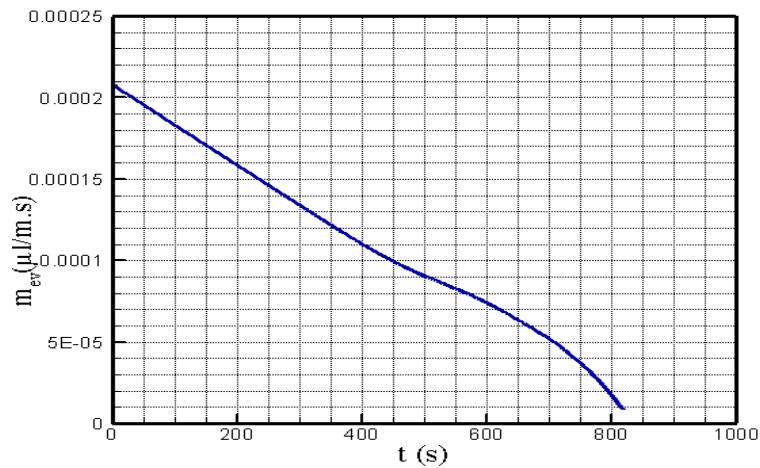


Fig.4. Evolution of the evaporated density over time: $T_{amb} = 21 \text{ }^\circ\text{C}$ and $H = 50 \%$

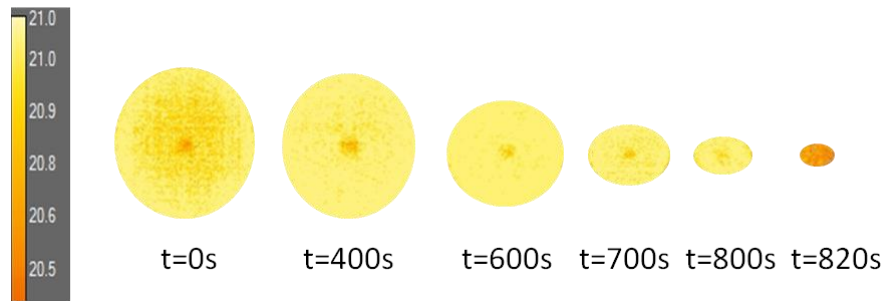


Fig.5. Snapshots from infrared video camera of evaporation process of water drop until the total disappearance of drop: $T_{amb} = 21 \text{ }^\circ\text{C}$ and $H = 50 \%$

3.2 Study of the interaction between drops during evaporation

Because in most industrial applications of the evaporation of liquid drops the latter are close to each other, it is important to study the phenomenon of their interaction during the evaporation process by considering the symmetrical configuration of a central drop surrounded by others (Conf (b)). Thus, the aim of our investigation is to study the effect of the interaction between the neighboring drops on the evaporation of the central drop. Using the syringe, we deposited these drops, separated at a relatively small distance ($d = 0.2 \text{ mm} \pm 0.02 \text{ mm}$), on the substrate. Their evaporation is done under the same conditions as the configuration of a single drop (Conf (a)).

3.2.1 Description of the phenomenon

The disposition of drops is described in Figure (6-1): 4 drops at the extremity (E_1, E_2, E_3, E_4), 2 drops at the center (C_2, C_3) and 1 central drop C_1 .

In Figure (6-2), we present a series of images taken by an infrared camera. These images show the evolution of the drops size as a function of time. They also demonstrate that the evaporation of the drops at the extremities (E_1, E_2) was faster, compared to that of the drops at the center (C_2 and C_3), particularly the central drop.

At $t = 3 \text{ s}$, the corresponding photo reveals that the diameter of the drops remained constant, which does not necessarily mean the absence of evaporation that can also take place in constant contact line mode.

At $t = 1200 \text{ s}$, a reduction in both the drop diameter and size occurred at the extremities (E_1, E_2, E_3, E_4) which have already reached the constant contact angle mode (Stade 2) demonstrated Figure 3. However, the minimization of the diameter of the drops at the center (C_2, C_3), particularly the central drop (C_1), was not remarkably observed but that does not necessarily mean the absence of evaporation. The evaporation can take place in a constant contact line mode (Stade 1). This highlights the interaction of the central drop with its neighbors. This result may be explained by changing local conditions in the vicinity of the central drop C_1 . The relative humidity, in proximity close to the gas-liquid interface of the central drop, increased due to evaporation of neighboring drops, which saturated the air surrounding the central drop and therefore reduced the density evaporated at the gas-liquid interface of this drop. From the fore-mentioned results, we may deduce that the evaporation of the central drop was delayed by that of the neighboring drops: The drops disappeared from the end towards the center (corresponding pictures at times $t = 1300 \text{ s}$, $t = 1600 \text{ s}$ and $t = 1700 \text{ s}$).

Figure 7 shows that the life of the central drop is pretty meadows 1760 s. Comparing the kinetics of evaporation of this drop to that of a single drop (Fig.5), we can conclude that the phenomenon of interaction reduces the lifetime of the drop of 51 %.

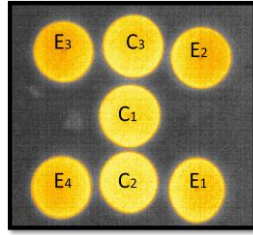


Fig.6-1. The description of drops arrangement

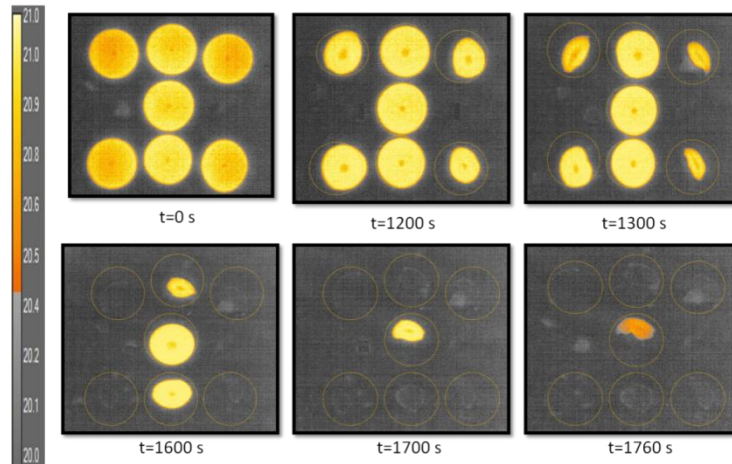


Fig.6-2. Snapshots of evaporation process over time: $T_{amb} = 21 \text{ }^\circ\text{C}$ and $H = 50 \%$ of the drops close to each other ($d = 0.2 \text{ mm} \pm 0.02 \text{ mm}$) taken by infrared video camera

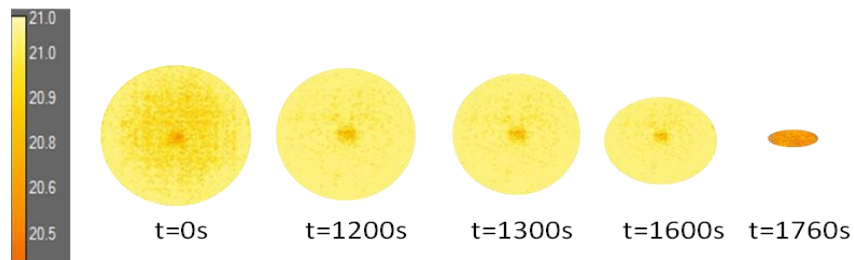


Fig.7. Snapshots of the evaporation process of water central drop until its total disappearance: $T_{amb} = 21 \text{ }^\circ\text{C}$ and $H = 50 \%$ taken by infrared video camera

3.2.2 Effect of the interaction between drops on evaporation

In this section, we will study the influence of interaction on the evaporation process by comparing the two following configurations: Conf (a): a single drop deposited on the substrate (single drop) and Conf (b): a drop surrounded by 6 other drops.

Figure 8 illustrates the evolution of the drop volume over time for both configurations. We note that the volume of the single drop (conf (a)) decreased more rapidly than that of the surrounded drop (conf (b)).

The life time of the drop deposited on a substrate and surrounded by six other drops close to each other (configuration (b)) was twice more than that of the drop deposited separately on the substrate (configuration (a)). This result shows that the interaction between the drops resulted in the central drop evaporation, which confirms the result observed in Figure 6.

We can conclude that, if the drop is surrounded by other neighbors, the volume will be reduced by 55%, for 850s, compared to the case of an isolated drop

Figure 9 and Figure 10 show the variations in the drop diameter and contact angle over time for both configurations (a) and (b). From these figures, we notice that both the central drop (conf (b)) and the single drop (conf (a)) evaporated according to the same evaporation mode.

Figure 11 depicts the evolution of the evaporated drop density over time for both configurations (a) and (b) and shows the effect of the phenomenon of interaction on evaporation.

The corresponding curve for the configuration (a): (single drop), takes a maximum value at $t = 0$ s. Then, it decreases over time, against the values of the density shown in configuration (b): (gout surrounded), are void at the beginning of evaporation and then increases over time.

In fact, at the beginning of evaporation, the central drop evaporated density was relatively negligible and drops were still very close to each other, which delayed the central drop evaporation. Obviously, it was not the same case for a single drop where evaporation was triggered at $t = 0$ s. Then, the evaporated density began to increase with the decrease of the neighboring drops influence. This can be explained mainly by the fact that the neighboring drops increased humidity at the air liquid interface of the central drop. Thus, the complete disappearance of the neighboring drops decreased the humidity nearby the central drop, which accelerated considerably its evaporation.

To examine the influence of the distance between the different drops on the kinetics of the central drop evaporation, we plotted the curves presented in Figure 12 which demonstrates the evolution of the central drop volume for three configurations: $d = 0.2$ mm, $d = 7$ mm and $d = 15$ mm (d is the distance between two successive drops). From this figure, it is noted that the volume of central drop decreased considerably by rising the distance (d) between the drops.

Indeed, the increase of the distance d between the drops induces:

- The increase in the volume of air surrounding the central drop.
- The decrease of humidity around the liquid-gas interface of the central drop.

Therefore, this evaluation shows that the interaction phenomenon between the drops was reduced by increasing the distance d .

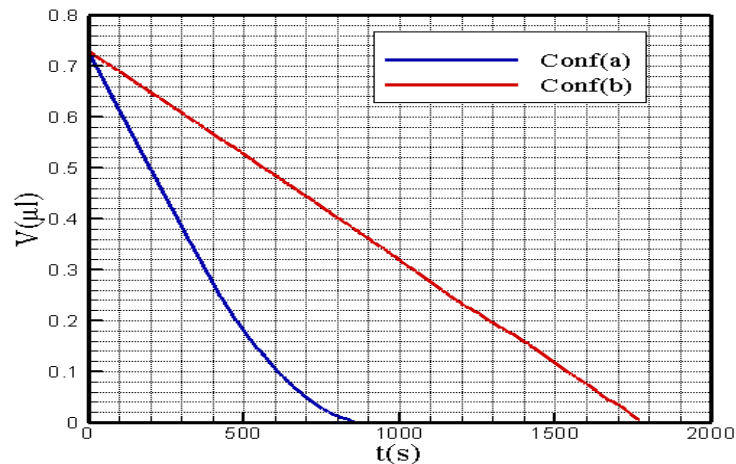


Fig.8. Variations in the drop volume as function of time for both configurations: Conf(a) : a single drop and Conf(b) : a drop surrounded by other drops : $T_{amb} = 21$ ° C and $H = 50$ %

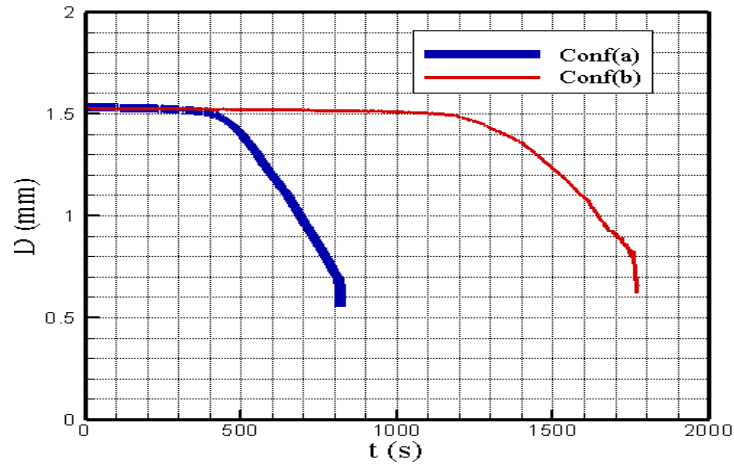


Fig.9. Variations in the drop diameter as function of time for both configurations: Conf(a) : a single drop and Conf(b) : a drop surrounded by other drops: $T_{amb} = 21^\circ \text{C}$ and $H = 50\%$

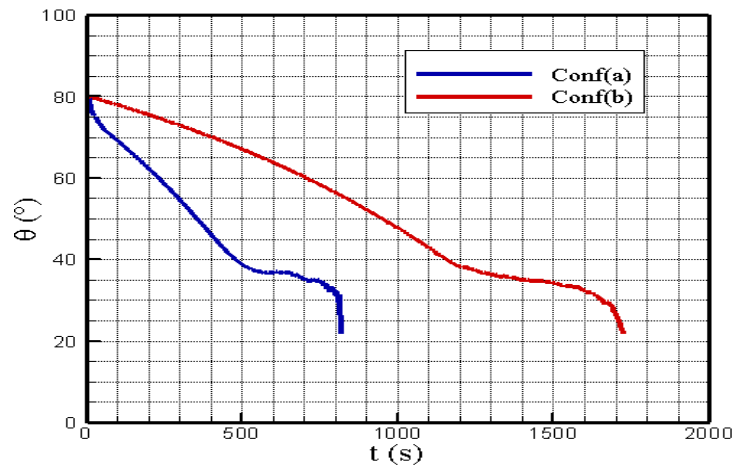


Fig.10. Variations in the drop contact angle as function of time for both configurations: Conf(a) : a single drop and Conf(b) : a drop surrounded by other drops: $T_{amb} = 21^\circ \text{C}$ and $H = 50\%$

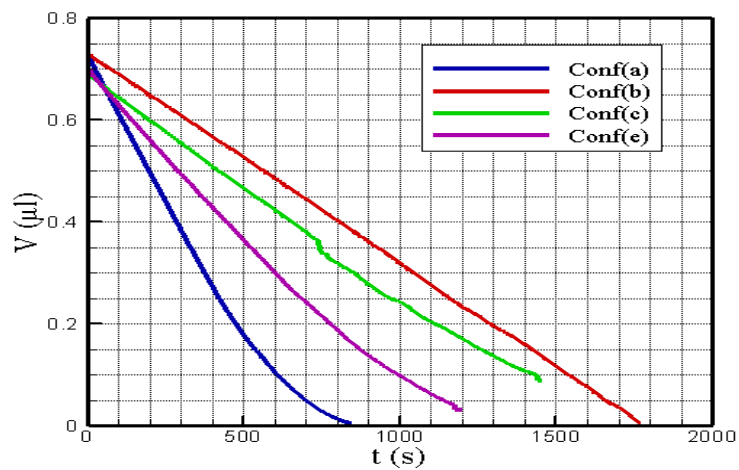


Fig.11. Evolution of the evaporated density over time for both configurations: Conf(a) : a single drop and Conf(b) : a drop surrounded by other drops: $T_{amb} = 21^\circ \text{C}$ and $H = 50\%$

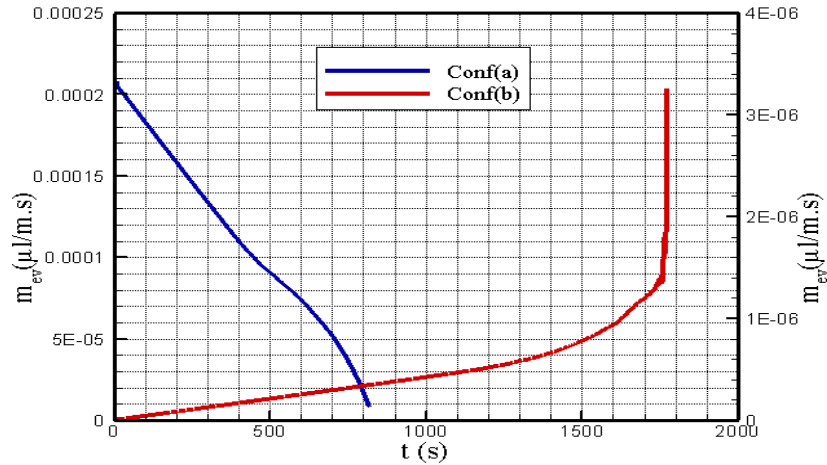


Fig.12. Variations in the drop volume as function of time for the four studied configurations: Conf (a): a single drop, Conf (b): $d = 0.2$ mm, Conf (c): $d = 7$ mm and Conf (e): $d = 15$ mm at $T_{amb} = 21$ ° C and $H = 50$ %

4. Summary of the results

The obtained results are summarized in (Table 1) in which we compare—the findings of a single drop (Conf (a)) with those of a surrounded drop in terms of the drop life time and volume. We considered the three configurations (Conf (b), Conf (c) and Conf (e)) by changing the distance between the drops. From this table, we can conclude that the volume of the surrounded drop was reduced, in 850s, by 55%, in configuration Conf (b), by 43% in configuration Conf (c) and by 23% in configuration Conf (e), compared to the case of a single drop. These results prove that the interaction phenomenon between the drops became less important by increasing the distance between the drops.

Tab.1. Summary table

	Single drop ($V_0 = 0.7 \mu\text{l}$) : Conf(a)	Drop surrounded by other drops ($V_0 = 0.7 \mu\text{l}$)		
		Conf (b) : $d = 0.2$ mm	Conf(c) : $d = 7$ mm	Conf (e) : $d = 15$ mm
The life expectancy of the drop (s)	850	1770	1650	1250
$V_{rest}(t = 850 \text{ s}) (\mu\text{l})$	0	0.383	0.302	0.161
$\frac{\Delta V(850s)}{V_0} (\%)$	100	45	56	77

With:

V_0 : presents the initial volume of drop: $V_0 = 0.7 \mu\text{l}$

$V_{rest}(t = 850 \text{ s})$: denotes the volume remaining at the instant $t = 850 \text{ s}$

$\Delta V(850 \text{ s}) (\mu\text{l})$: corresponds to the evaporated liquid during $\Delta t = 850 \text{ s}$

$\frac{\Delta V(850s)}{V_0} (\%)$: stands for the percentage of the evaporated liquid during $\Delta t = 850s$

The comparison time: $t = 850s$ is that of the total evaporation of the single drop.

5. Conclusion

In this research work, we highlighted the importance of the neighborhood effect on the evaporation of a water drop. From this study, we can conclude that:

- For drops which are very close to each other ($d = 0.2$ mm), the total evaporation can be minimized by 55% compared to that of an isolated drop. This reduction is mainly due to the increase of humidity near the drops.
- To decrease the effect of proximity on evaporation, the distance (d) between the drops must be increased.
- The variation of the distance between the neighboring drops allowed controlling the evaporation kinetics in cases where standard control parameters, such as humidity or substrate temperature, were out of control.
- This finding is important to optimize many industrial applications, such as spray drying, fuel injection in combustion engines, etc.

Nomenclatures

c	molar concentration, [mol/m^3].	
D	diameter, [mm].	<i>Greek symbols</i>
d	distance between two successive drops, [mm].	θ contact angle.
H	relative humidity.	<i>Subscripts</i>
m_{ev}	evaporated density, [$\mu\text{l}/(\text{m}\cdot\text{s})$].	0 initial.
T	temperature, [C].	amb environmental condition.
t	time, [s].	rest remaining.
V	volume, [μl].	sat saturated.

References

- [1] Wang, W. et al. Scanning force microscopy of 665 DNA molecules elongated by convective fluid flow in an evaporating 666 droplet. *Biophys. J.* 75, (1998), 513–520. 667.
- [2] Chopra, M. et al. DNA 668 molecular configurations in an evaporating droplet near a glass surface. *J. Rheol.* 47, (2003), 1111.
- [3] Kawase, T. et al. Inkjet 659 printed via-hole interconnections and resistors for all-polymer 660 transistor circuits. *Adv. Mater.* 661, (2001), 13, 1601–1605.
- [4] de Gans, B.J. et al. Inkjet printing 662 of polymers: State of the art and future developments. *Adv. Mater.* 663 (2004), 16, 203–213.
- [5] Saito, M. et al. Evaporation and combustion of a 671 single fuel droplet in acoustic fields. *Fuel* (1994), 73, 349–353. 672.
- [6] Park, C.W. et al. Evaporation-combustion affected by 673 in-cylinder, reciprocating porous regenerator. *J. Heat Transfer* (2002), 674 124, 184–194.
- [7] MURKO, V. I. et al. Investigation of the spraying mechanism and combustion of the suspended coal fuel. *J. Thermal Science* 19, (2015), 243-251.
- [8] Bar-Cohen, A. et al. Direct liquid cooling of high flux micro and nano electronic components, Proc. *IEEE* 94 (8) (2006) 1549–1570.
- [9] CHEN, Z. et al. Numerical simulation of single-nozzle large scale spray cooling on drum wall. *J. Thermal Science* 22, (2018), 359-370.

- [10] David, S. et al. Experimental investigation of the effect of thermal properties of the substrate in the wetting and evaporation of sessile drops, *Colloids surf. A* 298, (2007), 108-114..
- [11] Dunn, G. et al. The strong influence of substrate conductivity on droplet evaporation, *Journal of Fluid Mechanics*. March. 623, (2009), 329-351.
- [12] Lopes, M. C. et al. Influence of the substrate thermal properties on sessile droplet evaporation: Effect of transient heat transport, *Colloids Surfaces A: Physicochem. Eng. Aspects* 432, (2013), 64–70.
- [13] Strotos, G. et al. Numerical investigation on the evaporation of droplets depositing on heated surfaces at low weber numbers, *International journal of heat and mass transfer* 51, (2008), 1516-1529.
- [14] Ait Saada, M. et al. Evaporation of a sessile drop with pinned or receding contact line on a substrate with different thermophysical properties, *International journal of heat and mass transfer* 58, (2013), 197-208.
- [15] Picknett, R.G. et al. The evaporation of sessile or pendant drops in still air, *J. Colloid Interface Sci.* 61, (1977), 336–350.
- [16] Shanahan, M.E.R. Simple theory of stick–slip wetting hysteresis, *Langmuir* 11, (1995), 1041–1043.
- [17] Orejon, D. et al. Stick–slip of evaporating droplets: substrate hydrophobicity and nanoparticle concentration, *Langmuir* 27 (2011) 12834–12843.
- [18] Bourgès-Monnier, C. et al. Influence of evaporation on contact angle, *Langmuir* 11, (1995), 2820–2829.
- [19] Bormashenko, E. et al. Evaporation of droplets on strongly and weakly pinning surfaces and dynamics of the triple line, *Colloids Surf. A* 385, (2011), 235–240.
- [20] Moffat, J.R. et al. Effect of TiO₂ nanoparticles on contact line stick–slip behavior of volatile drops, *J. Phys. Chem. B* 113, (2009), 8860–8866.
- [21] Bodiguel H. et al. Stick–slip patterning at low capillary numbers for an evaporating colloidal suspension, *Langmuir* 26, (2010), 10758–10763.
- [22] Gui Lu. Et al. Internal flow in evaporating droplet on heated solid surface, *International journal of heat and mass transfer* 54 (2011° 4437-4447).
- [23] Kai Yang. Et al. A fully coupled numerical simulation of sessile droplet evaporation using Arbitrary Lagrangian-Eulerian formulation, *International journal heat and mass transfer* 70 (2014) 409-420.
- [24] Ouenzerfi, S. et al. Experimental droplet study of inverted Marangoni effect of a binary liquid mixture on a non-uniform heated substrate, *Langmuir* 32, (2016), 2378–2388.
- [25] Pin C. et al. Evaporation of Binary Sessile Drops: Infrared and Acoustic Methods To Track Alcohol Concentration at the Interface and on the Surface, *Langmuir* 32, (2016), 9836–9845.
- [26] Semenov, S. et al. Computer simulations of quasi-steady evaporation of sessile liquid droplets, *Prog. Coll. Pol. Sci. S* 138, (2011), 115–120.
- [27] Ruiz, O.E. et al. Evaporation of water droplets placed on a heated horizontal surface, *J. Heat Transfer – Trans. ASME* 124, (5), (2002), 854–863.
- [28] Murisic, N. et al. On evaporation of sessile drops with moving contact lines, *J. Fluid Mech.* 679, (2011), 219–246.
- [29] Hu, H. et al. Evaporation of a sessile droplet on a substrate, *J. Phys. Chem. B* 106, (6), (2002), 1334–1344.
- [30] Girard, F. et al. On the effect of Marangoni flow on evaporation rates of heated water drops, *Langmuir* 24, (17), (2008), 9207–9210.
- [31] Mollaret, R. et al. Experimental and numerical investigation of the evaporation into air of a drop on a heated surface, *Chem. Eng. Res. Des.* 82, (4), (2004), 471–480.
- [32] Widjaja, E. et al. Numerical study of vapor phase diffusion driven sessile drop evaporation. *Computers and chemical Engineering* 32, (2008), 2169-2178.
- [33] Galvin, K.P. A conceptually simple derivation of the Kelvin equation, *Chem. Eng. Sci.* 60, (2005), 4659.

Paper submitted: 06. April 2018
Paper revised 07. June 2018
Paper accepted: 09. June 2018